Efficient dual-wavelength diode-end-pumped laser with a diffusion-bonded Nd:YVO_4/Nd:$GdVO_4$ crystal

Y. J. Huang,[1] H. H. Cho,[1] Y. S. Tzeng,[1] H. C. Liang,[2] K. W. Su,[1] and Y. F. Chen[1,3]*

[1]*Department of Electrophysics, National Chiao Tung University, Hsinchu 30010, Taiwan*
[2]*Institute of Optoelectronic Science, National Taiwan Ocean University, Keelung 20224, Taiwan*
[3]*Department of Electronics Engineering, National Chiao Tung University, Hsinchu 30010, Taiwan*
[*]*yfchen@cc.nctu.edu.tw*

Abstract: A new type of diffusion-bonded Nd:YVO_4/Nd:$GdVO_4$ hetero-composite crystal is originally designed and applied to diode-end-pumped laser for achieving an efficient dual-comb picosecond operation with self-mode locking for the first time. As high as 1.1 W of the total average output power at 1063.18 and 1064.37 nm is generated under an incident pump power of 5.1 W. The corresponding mode-locked pulse width is 42 ps at a pulse repetition rate of 3.82 GHz. Through the optical beating between two carrier frequencies of each spectral component, a train of ultrashort pulses with sub-terahertz repetition rate is further generated with the effective duration of down to 1.6 ps.

©2015 Optical Society of America

OCIS codes: (140.3380) Laser materials; (140.4050) Mode-locked lasers; (140.3530) Lasers, neodymium; (140.3480) Lasers, diode-pumped; (140.3580) Lasers, solid-state.

References and links

1. G. Q. Xie, D. Y. Tang, H. Luo, H. J. Zhang, H. H. Yu, J. Y. Wang, X. T. Tao, M. H. Jiang, and L. J. Qian, "Dual-wavelength synchronously mode-locked Nd:CNGG laser," Opt. Lett. **33**(16), 1872–1874 (2008).
2. D. Li, X. Xu, J. Meng, D. Zhou, C. Xia, F. Wu, and J. Xu, "Diode-pumped continuous wave and Q-switched operation of Nd:$CaYAlO_4$ crystal," Opt. Express **18**(18), 18649–18654 (2010).
3. A. Agnesi, F. Pirzio, G. Reali, A. Arcangeli, M. Tonelli, Z. Jia, and X. Tao, "Multi-wavelength Nd:GAGG picosecond laser," Opt. Mater. **32**(9), 1130–1133 (2010).
4. Y. Zhao, S. Zhuang, X. Xu, J. Xu, H. Yu, Z. Wang, and X. Xu, "Anisotropy of laser emission in monoclinic, disordered crystal Nd:LYSO," Opt. Express **22**(3), 2228–2235 (2014).
5. G. Alombert-Goget, A. Brenier, Y. Guyot, A. Labruyère, B. Faure, and V. Couderc, "Thermally driven dual-frequency Q-switching of Nd:$YGd_2Sc_2Al_2GaO_{12}$ ceramic laser," Opt. Express **22**(9), 10792–10799 (2014).
6. H. Yu, J. Liu, H. Zhang, A. A. Kaminskii, Z. Wang, and J. Wang, "Advances in vanadate laser crystals at a lasing wavelength of 1 micrometer," Laser Photonics Rev. **8**(6), 847–864 (2014).
7. F. Hanson, "Improved laser performance at 946 and 473 nm from a composite Nd:$Y_3Al_5O_{12}$ rod," Appl. Phys. Lett. **66**(26), 3549–3551 (1995).
8. M. Tsunekane, N. Taguchi, T. Kasamatsu, and H. Inaba, "Analytical and experimental studies on the characteristics of composite solid-state laser rods in diode-end-pumped geometry," IEEE J. Sel. Top. Quantum Electron. **3**(1), 9–18 (1997).
9. Y. T. Chang, Y. P. Huang, K. W. Su, and Y. F. Chen, "Comparison of thermal lensing effects between single-end and double-end diffusion-bonded Nd:YVO_4 crystals for $^4F_{3/2}\rightarrow{}^4I_{11/2}$ and $^4F_{3/2}\rightarrow{}^4I_{13/2}$ transitions," Opt. Express **16**(25), 21155–21160 (2008).
10. D. Kracht, R. Wilhelm, M. Frede, K. Dupré, and L. Ackermann, "407 W end-pumped multi-segmented Nd:YAG laser," Opt. Express **13**(25), 10140–10144 (2005).
11. Y. J. Huang and Y. F. Chen, "High-power diode-end-pumped laser with multi-segmented Nd-doped yttrium vanadate," Opt. Express **21**(13), 16063–16068 (2013).
12. R. Feldman, Y. Shimony, and Z. Burshtein, "Passive Q-switching in Nd:YAG/Cr^{4+}:YAG monolithic microchip laser," Opt. Mater. **24**(1–2), 393–399 (2003).
13. J. Šulc, H. Jelinková, K. Nejezchleb, and V. Škoda, "Nd:YAG/V:YAG microchip laser operating at 1338 nm," Laser Phys. Lett. **2**(11), 519–524 (2005).
14. B. Zhang, N. Du, J. He, S. Liu, J. Yang, and H. Huang, "355-nm UV generation by intracavity frequency tripled passively Q-switched Nd:YAG/Cr^{4+}:YAG laser," IEEE Photonics Technol. Lett. **23**(10), 612–614 (2011).
15. S. Zhu, Z. Chen, Z. Chen, W. Jiang, S. Wang, Q. Zhang, H. Yin, Z. Li, A. Li, and Y. Chen, "A LD side-pumped deep ultraviolet laser at 266 nm by using a Nd:YAG/Cr^{4+}:YAG/YAG composite crystal," Opt. Laser Technol. **63**, 24–28 (2014).

#246132 Received 15 Jul 2015; revised 1 Sep 2015; accepted 2 Sep 2015; published 4 Sep 2015

16. Y. J. Huang, Y. S. Tzeng, C. Y. Tang, and Y. F. Chen, "Efficient dual-wavelength synchronously mode-locked picosecond laser operating on the $^4F_{3/2} \rightarrow {}^4I_{11/2}$ transition with compactly combined dual gain media," IEEE J. Sel. Top. Quantum Electron. **21**(1), 1100107 (2015).
17. Y. J. Huang, Y. S. Tzeng, H. H. Cho, and Y. F. Chen, "Effect of spatial hole burning on a dual-wavelength mode-locked laser based on compactly combined dual gain media," Photon. Res. **2**(6), 161–167 (2014).
18. C. J. Flood, D. R. Walker, and H. M. van Driel, "Effect of spatial hole burning in a mode-locked diode end-pumped Nd:YAG laser," Opt. Lett. **20**(1), 58–60 (1995).
19. B. Braun, K. J. Weingarten, F. X. Kärtner, and U. Keller, "Continuous-wave mode-locked solid-state lasers with enhanced spatial hole burning," Appl. Phys. B **61**(5), 429–437 (1995).
20. Y. J. Huang, Y. P. Huang, H. C. Liang, K. W. Su, Y. F. Chen, and K. F. Huang, "Comparative study between conventional and diffusion-bonded Nd-doped vanadate crystals in the passively mode-locked operation," Opt. Express **18**(9), 9518–9524 (2010).
21. Y. F. Chen, Y. J. Huang, P. Y. Chiang, Y. C. Lin, and H. C. Liang, "Controlling number of lasing modes for designing short-cavity self-mode-locked Nd-doped vanadate lasers," Appl. Phys. B **103**(4), 841–846 (2011).
22. A. Lagatsky, C. Brown, and W. Sibbett, "Highly efficient and low threshold diode-pumped Kerr-lens mode-locked Yb:KYW laser," Opt. Express **12**(17), 3928–3933 (2004).
23. G. Q. Xie, D. Y. Tang, L. M. Zhao, L. J. Qian, and K. Ueda, "High-power self-mode-locked Yb:Y_2O_3 ceramic laser," Opt. Lett. **32**(18), 2741–2743 (2007).
24. H. C. Liang, R. C. C. Chen, Y. J. Huang, K. W. Su, and Y. F. Chen, "Compact efficient multi-GHz Kerr-lens mode-locked diode-pumped Nd:YVO_4 laser," Opt. Express **16**(25), 21149–21154 (2008).
25. H. C. Liang, Y. J. Huang, W. C. Huang, K. W. Su, and Y. F. Chen, "High-power, diode-end-pumped, multigigahertz self-mode-locked Nd:YVO_4 laser at 1342 nm," Opt. Lett. **35**(1), 4–6 (2010).
26. Y. J. Huang, Y. S. Tzeng, C. Y. Tang, Y. P. Huang, and Y. F. Chen, "Tunable GHz pulse repetition rate operation in high-power TEM_{00}-mode Nd:YLF lasers at 1047 nm and 1053 nm with self mode locking," Opt. Express **20**(16), 18230–18237 (2012).
27. C. L. Wang and C. L. Pan, "Tunable multiterahertz beat signal generation from a two-wavelength laser-diode array," Opt. Lett. **20**(11), 1292–1294 (1995).

1. Introduction

Lasers emitting two spectral lines are highly attractive for a large number of applications such as biomedicine, precision metrology, differential analysis, pump-probe measurement, spectroscopic study, and so on. With a significant progress in the growth of laser materials, a series of disordered crystals has been extensively fabricated and identified to generally possess multiple fluorescent peaks with comparable spectral intensity. Thanks to this distinctive property, directly utilizing the Nd- or Yb-doped disordered crystals as the active media becomes one of the most promising tactics for constructing a dual-wavelength laser in the continuous-wave, Q-switched, as well as mode-locked operations [1–5]. Nevertheless, the critical issue for such a kind of light source to be practically used is the uncontrollable intensity ratio between each emission component.

The Nd-doped vanadate crystal is characterized by a high absorption coefficient, a large stimulated emission cross section, and natural birefringence that is favorable for building an efficient diode-pumped solid-state laser with linearly polarized output [6]. Usually, the Nd-doped vanadate laser is designed to operate with π-polarized emission thanks to the larger stimulated emission cross section as compared with the σ-polarization. However, its smaller Stark splitting and more compact multiple transitions lead to a less spiky fluorescent profile, typically causing the lasing output with a single emission line around 1.06 μm. Therefore, it is practically important and highly desirable to develop a promising method for achieving the dual-wavelength emission in a π-polarized Nd-doped vanadate laser.

The maturity of the diffusion bonding technology is another impressive development benefiting from advances in manufacturing optical materials. This technique has led the existing gain media to possess additional functions including an effective heat sink for efficient removal of the heat generated in the laser media [7–11] or an integration of the saturable absorber for constructing a passively Q-switched laser [12–15]. Motivated by our previous idea of compactly combined dual gain media [16], in this work we originally design a new type of composite crystal by diffusion bonding Nd:YVO_4 and Nd:$GdVO_4$ materials for the first time. The fluorescent spectrum is measured to show the large feasibility of the developed hetero-composite crystal for efficient π-polarized dual-wavelength emission in a diode-end-pumped solid-state laser. With a self-mode locking, the total average output power of up to 1.1 W for the developed dual-comb laser at 1063 and 1064 nm is efficiently

#246132 Received 15 Jul 2015; revised 1 Sep 2015; accepted 2 Sep 2015; published 4 Sep 2015

generated with the mode-locked pulse width of 42 ps at a pulse repetition rate of 3.82 GHz. We further find that the temporal overlapping between each group causes the formation of a series of optically beat pulses. Two individual Nd:YVO_4 and Nd:$GdVO_4$ crystals with the same specifications are also prepared and placed in close contact for making a comparison to reveal that the designed diffusion-bonded Nd:YVO_4/Nd:$GdVO_4$ crystal is a promising device in constructing a high-quality dual-wavelength diode-end-pumped solid-state laser.

2. Experimental setup

The experimental configuration of the diode-end-pumped dual-comb self-mode-locked Nd:YVO_4/Nd:$GdVO_4$ laser is schematically depicted in Fig. 1(a). A 6-W fiber-coupled laser diode at 808 nm with a core diameter of 200 μm and a numerical aperture of 0.22 was employed as the pump source. A pair of plano-convex coupling lenses was used to reimage the fiber end into the laser crystal with a spot radius of approximately 100 μm. The system of coupling lenses could be finely adjusted to control the emission intensity between two spectral components through the parameter z_0, which is defined as the distance from the entrance face of the diffusion-bonded crystal to the waist location of the pump beam inside the gain medium [16,17]. The input mirror was a plano-concave mirror with the radius of curvature of 1000 mm. It was coated for antireflection (AR, $R < 0.25\%$) at 808 nm on the plane side and coated for high reflection ($R > 99.8\%$) at 1.06 μm as well as high transmission ($T > 95\%$) at 808 nm on the concave side. The gain medium was a hetero-composite crystal fabricated by diffusion bonding the Nd:YVO_4 and Nd:$GdVO_4$ materials (manufactured by Innowit Co., Ltd.), as displayed in Fig. 1(b). The parallelism of the diffusion-bonded crystal specified by the supplier was better than 20 arc seconds. The doping concentration and the length for the Nd:YVO_4 crystal were designed as 0.2 at.% and 3 mm for the pump absorption at 808 nm to be around 50%, and the residual pump light was absorbed by the Nd:$GdVO_4$ crystal with the doping concentration of 0.5 at.% and the length of 7 mm. Another reason for choosing the length of the Nd:YVO_4 part to be 3 mm is to ensure the fundamental transverse mode oscillation without greatly defocusing (i.e., large z_0) to get power-equalized condition [17].

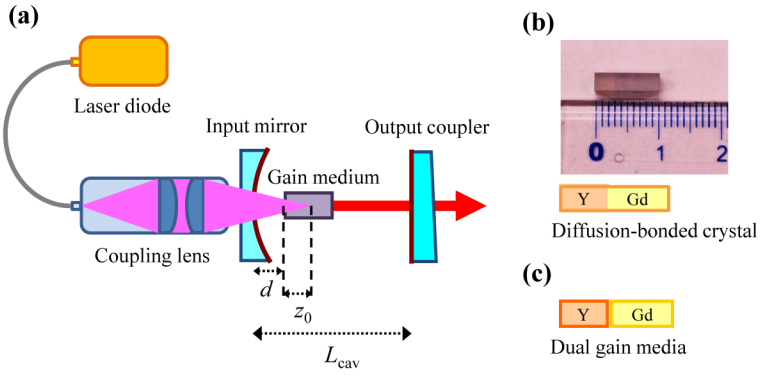

Fig. 1. (a) Experimental setup of the diode-end-pumped dual-comb self-mode-locked Nd:YVO_4/Nd:$GdVO_4$ laser; Schematic configurations for the (b) diffusion-bonded crystal (Nd:YVO_4/Nd:$GdVO_4$ hetero-composite crystal), and (c) the dual gain media structure.

The transverse cross section of the gain medium was 3 mm × 3 mm, and the crystallographic *c* axes for both materials were oriented to be parallel to each other. Both facets of the diffusion-bonded crystal were coated for antireflection at the pump and lasing wavelengths. The composite crystal was wrapped with indium foil and mounted in a water-cooled copper holder at the temperature of 18°C to effectually dissipate the generated heat. To avoid unwanted etalon effect, a flat wedged mirror with reflectivity of 95% at 1.06 μm was employed as the output coupler. The geometrical length of the laser cavity L_{cav} was set to be 27 mm. As a result, the optical cavity length is calculated as 39.3 mm by considering the

#246132 Received 15 Jul 2015; revised 1 Sep 2015; accepted 2 Sep 2015; published 4 Sep 2015

refractive indices of the laser materials, corresponding to the free spectral range of 3.82 GHz. The degree of the spatial hole burning effect could be adjusted by the separation *d* between the input mirror and the active medium in a standing-wave cavity [18–20], and this parameter was chosen to be 8 mm for acquiring comparable mode-locked pulse durations at 1063 and 1064 nm [21].

The real-time temporal behavior of the mode-locked pulses was captured by a high-speed InGaAs photodetector (Electro-Optics Technology, ET 3500) with a rise time of 35 ps, and the received signal was sent to a digital oscilloscope (Teledyne LeCroy, WaveMaster 820Zi-A) with an electrical bandwidth of 20 GHz and a sampling interval of 25 ps. The output signal of the photodetector was also delivered to a RF spectrum analyzer (Agilent, 8563EC) with a bandwidth of 26.5 GHz. The fine structure of the mode-locked pulses was measured with the first-order autocorrelation by a Fourier spectrum system (Advantest, Q8347) based on a Michelson interferometer. Moreover, the optical spectrum could be obtained by performing the fast Fourier transform over the interferogram with the resolution of 0.003 nm. Since the mode spacing for the free spectral range of 3.82 GHz is about 0.015 nm, the longitudinal modes could be clearly resolved. The wavelength accuracy specified by the manufacturer is within ± 0.01 nm. We also employed a commercial autocorrelator (APE pulse check, Angewante Physic and Elektronik GmbH) with non-collinear configuration to record the second-order autocorrelation of the mode-locked pulses and found the excellent resemblance with the first-order autocorrelation trace for the experimental results.

3. Experimental results and discussion

First of all, the normalized room-temperature polarization-resolved fluorescent spectra for the diffusion-bonded Nd:YVO_4/Nd:$GdVO_4$ crystal were measured in Figs. 2(a) and 2(b) for the π- and σ-polarization components. As a comparison, these figures also show the normalized polarization-resolved fluorescent spectra for the Nd:YVO_4 and Nd:$GdVO_4$ crystals, respectively. For the π-polarization, it can be determined undoubtedly that the dual fluorescent peaks at 1064 and 1063 nm with nearly comparable spectral intensity in the diffusion-bonded Nd:YVO_4/Nd:$GdVO_4$ crystal are contributed by the individual Nd:YVO_4 and Nd:$GdVO_4$ parts,

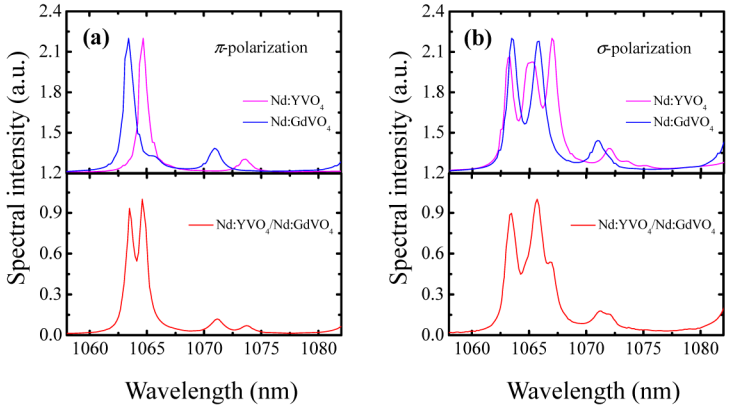

Fig. 2. Fluorescent spectra of the Nd:YVO_4, Nd:$GdVO_4$, and diffusion-bonded Nd:YVO_4/Nd:$GdVO_4$ crystals for the (a) π- and (b) σ-polarization components.

respectively. On the other hand, the relatively structured σ-polarizations of the individual Nd:YVO_4 and Nd:$GdVO_4$ crystals are found to both contribute to the formation of dual fluorescent peaks at 1063 and 1066 nm with similar spectral intensity in the diffusion-bonded Nd:YVO_4/Nd:$GdVO_4$ crystal for this polarization component. Since the stimulated emission cross section for the π-polarization is larger than that for the σ-polarization in the Nd-doped

#246132 Received 15 Jul 2015; revised 1 Sep 2015; accepted 2 Sep 2015; published 4 Sep 2015

vanadate material, in the following we will focus on the laser performance of the developed diffusion-bonded Nd:YVO_4/Nd:$GdVO_4$ crystal with the π-polarization at 1063 and 1064 nm.

Then, we experimentally confirmed that by finely tilting the gain medium and carefully adjusting the cavity alignment, a fairly stable continuous-wave self-mode-locked operation could be achieved. The combination of Kerr lensing and thermal lensing effects is regarded to be able to support the required nonlinearity for achieving stable self-mode locking in a solid-state laser configured with the diode-end-pumped scheme [22–26]. Figure 3(a) describes the dependence of the total average output power at 1.06 μm on the incident pump power under the optimally balanced dual-wavelength intensity, corresponding to z_0 = 2.5 mm. The pump threshold is around 0.55 W, and the maximum total average output power is found to reach 1.1 W under an incident pump power of 5.1 W. The optical spectrum under gain balancing is recorded in Fig. 3(b). The emission wavelengths for each spectral band are centered at 1063.18 and 1064.37 nm, respectively. The beam quality was measured to be $M^2 < 1.2$.

Typical oscilloscope traces of the dual-comb mode-locked pulses are illustrated in Figs. 4(a) and 4(b). Figure 4(a) shows the amplitude stability of the laser, and the fluctuation is

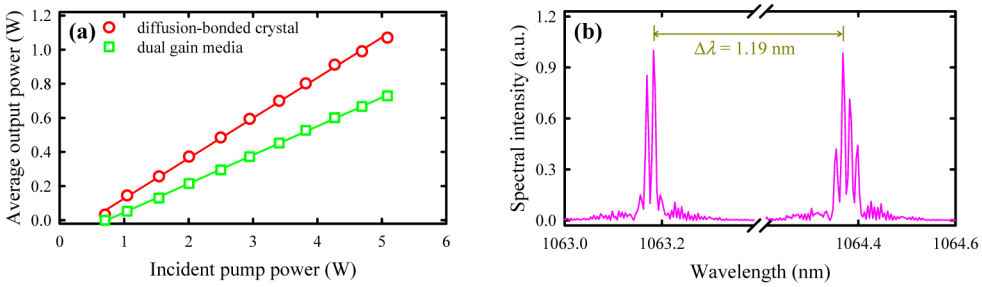

Fig. 3. (a) Average output powers versus the incident pump power for the diffusion-bonded Nd:YVO_4/Nd:$GdVO_4$ crystal and the dual gain media structure; (b) Optical spectrum for the dual-comb Nd:YVO_4/Nd:$GdVO_4$ laser.

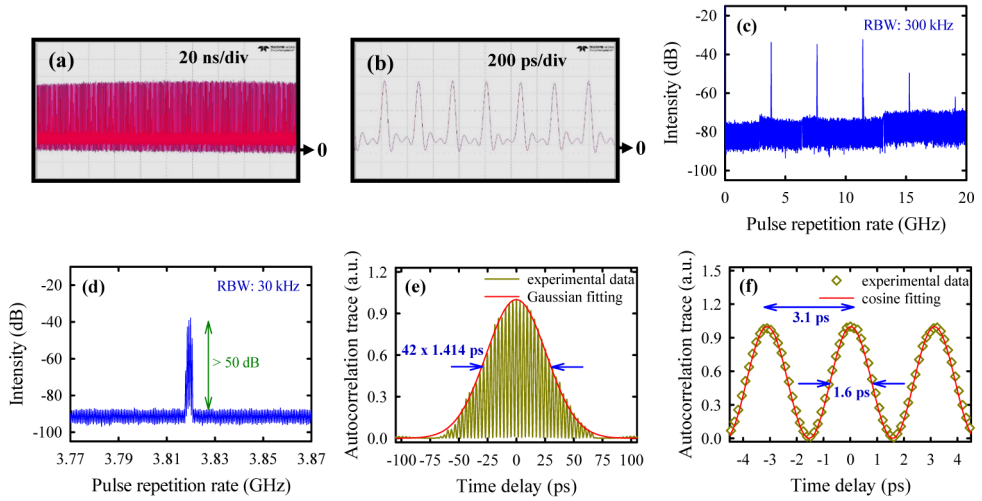

Fig. 4. Oscilloscope traces with the time span of (a) 200 ns and (b) 2 ns, RF spectra with the span of (c) 20 GHz and (d) 100 MHz, and autocorrelation traces with the time interval of (e) 210 ps and (f) 9 ps, for the dual-comb Nd:YVO_4/Nd:$GdVO_4$ laser.

experimentally found to be within ± 2%. No CW background was observed during the experiment. The pulse period, as can be deduced in Fig. 4(b), is 262 ps that agrees with the round-trip time determined by the optical cavity length of 39.3 mm. More importantly, only

#246132 Received 15 Jul 2015; revised 1 Sep 2015; accepted 2 Sep 2015; published 4 Sep 2015
(C) 2015 OSA

one mode-locked pulse is generated in a round-trip time scale, which shows an excellent synchronization between each spectral group. Figures 4(c) and 4(d) present the RF spectra of the dual-comb Nd:YVO_4/Nd:$GdVO_4$ laser, respectively. A number of harmonics equally spaced by the fundamental repetition rate of 3.82 GHz could be observed in Fig. 4(c), and the reductions in the amplitudes of the fourth and fifth harmonics are attributed to the limited bandwidth of the photodetector. The signal-to-noise level displayed in Fig. 4(d) is experimentally found to be larger than 50 dB, indicating a good stability of the laser. The excellent stability was also verified by observing the nearly invariant pulse shape and signal intensity of autocorrelation trace for the mode-locked pulses over one-hour-long examination. The autocorrelation trace of the dual-comb self-mode-locked laser is exhibited in Fig. 4(e). Assuming the temporal intensity follows a Gaussian-shaped profile, the pulse duration could thus be evaluated as 42 ps. Furthermore, a strong interference fringe with the strong modulation depth is observed in the autocorrelation trace as a result of the optical beating between two carrier frequencies of the pulses at 1063 and 1064 nm. Figure 4(f) illustrates the detailed characteristic of the interference fringe pattern. The optical beat frequency of 0.32 THz could be deduced from the pulse period of 3.1 ps, and it shows good agreement with the central wavelength separation $\Delta\lambda$ of 1.19 nm of the two spectral bands measured in Fig. 3(b). In terms of the cosine-like pulse shape, the effective pulse width of the optically beat wave could be inferred to exactly correspond to the FWHM duration of the experimentally measured autocorrelation trace [27]. As a result, the effective pulse duration is calculated to be as short as 1.6 ps, considerably narrower than the original Gaussian-shaped pulse of 42 ps.

Finally, we prepared and physically combined the individual AR-coated Nd:YVO_4 and Nd:$GdVO_4$ crystals in close contact with the identical specifications [17], as indicated in Fig. 1(c), for making a systematic comparison. It is experimentally found that the laser performance based on the dual gain media structure is relatively sensitive to the package process due to the parallelism uncertainty in aligning two separate crystals, although the oscilloscope traces, RF spectra, and autocorrelation traces under the optimal gain balancing for the dual gain media structure could be achieved to be nearly the same as those obtained from the diffusion-bonded Nd:YVO_4/Nd:$GdVO_4$ crystal. However, under the optimal gain balancing, the total average output power obtained from the dual gain media scheme is commonly found to be 30% lower than that achieved in the diffusion-bonded Nd:YVO_4/Nd:$GdVO_4$ crystal, as can be observed in Fig. 3(a). We think that the reduction of the total average output power is mainly attributed to the additional loss caused by the parallelism uncertainty during the package process of two separate crystals. According to the aforementioned results, we believe that the proposed diffusion-bonded hetero-composite Nd-doped crystal will find its practical usefulness in constructing a high-quality diode-end-pumped dual-wavelength solid-state laser with a large flexibility.

4. Conclusion

In summary, a novel diffusion-bonded Nd:YVO_4/Nd:$GdVO_4$ crystal has been successfully designed and fabricated with demonstration of high-quality dual-comb self-mode-locked operation in a diode-end-pumped solid-state laser at 1063 and 1064 nm for the first time. Under an incident pump power of 5.1 W, the total average output power of 1.1 W under the optimal gain balancing was efficiently generated with the mode-locked pulse width of 42 ps at a pulse repetition rate of 3.82 GHz. Experimental results further revealed that the temporal interference between two carrier frequencies of the dual-comb pulses leads to the generation of quasi-periodic fringe with the sub-terahertz repetition rate of 0.32 THz.

Acknowledgments

The authors thank the Ministry of Science and Technology for their financial support of this research under Contract No. MOST 103-2112-M-009-016-MY3.

#246132 Received 15 Jul 2015; revised 1 Sep 2015; accepted 2 Sep 2015; published 4 Sep 2015